

# Preparation and characterization of near-infrared region absorption enhancer carbon nanotubes hybrid materials

Peng Huang\*, Chunlei Zhang, Cheng Xu, Le Bao, Zhiming Li

Department of Bio-Nano Science and Engineering, National Key Laboratory of Nano/Micro Fabrication Technology, Key Laboratory for Thin Film and Microfabrication of Ministry of Education, Institute of Micro-Nano Science and Technology, Shanghai Jiao Tong University, 800 Dongchuan Road, Shanghai 200240, China

\*Corresponding author: [hhcht@sjtu.edu.cn](mailto:hhcht@sjtu.edu.cn)

## Abstract

This paper describes a simple strategy for covalently attaching silica-coated gold nanorods (sGNRs) onto the surface of multi-walled carbon nanotubes (MWNT) to fabricate hybrid nanostructures. The crosslinked reaction occurs through interaction of carboxyl groups on the MWNT with the amino silane coupling agent modified sGNRs. TEM, FT-IR spectroscopy, UV-vis spectroscopy, and Zeta potential analysis have been used to study the formation of MWNT/sGNRs nanostructure. Furthermore, MWNT/sGNRs hybrid material shows an excellent solubility in aqueous solution and an enhanced absorption in the near-infrared region. It should open up new possibilities in nanomedicine as multimodal photoacoustic and photothermal high-contrast molecular agent.

**Key Words:** gold nanorod, multi-walled carbon nanotube, preparation, characterization

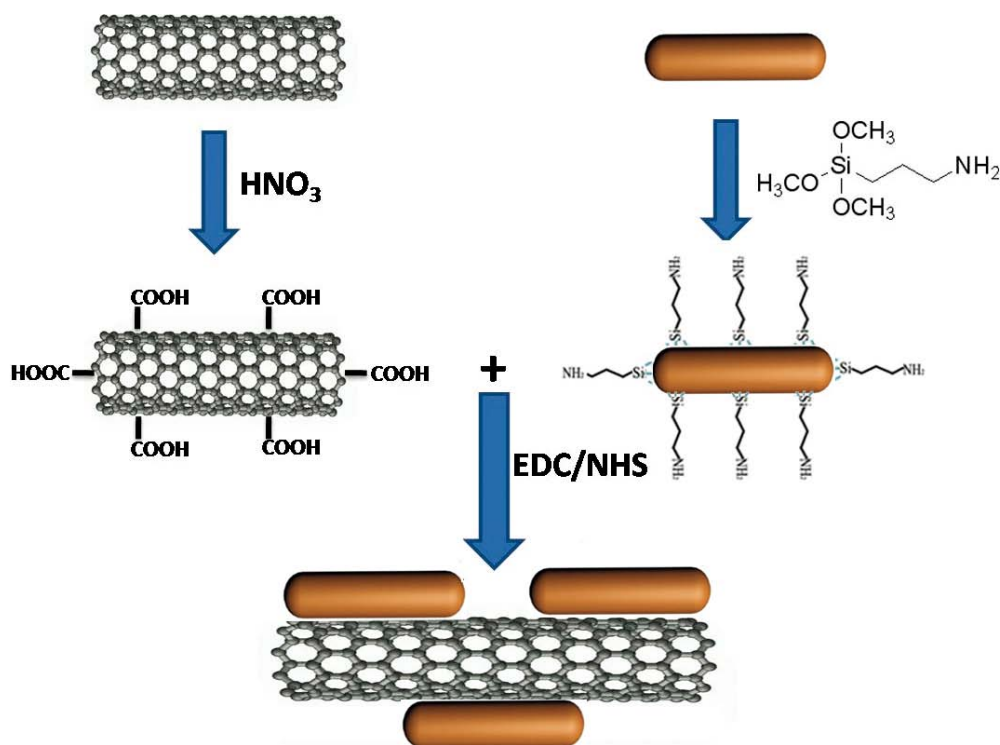
**Citation:** P. Huang, et al. Preparation and Characterization of Near-infrared region absorption enhancer carbon nanotubes hybrid materials. *Nano Biomed. Eng.* 2010, 2(4), 225-230. DOI: 10.5101/nbe.v2i4.p225-230.

## 1. Introduction

Carbon nanotubes (CNTs) have been intensively studied in recent years due to their unique structural, electrical, mechanical, optical, thermal and chemical properties [1-12]. In health-care industry, CNTs have shown promise as contrast agents for photoacoustic and photothermal imaging of tumours and infections because they offer high resolution and allow deep tissue imaging [13-16]. However, *in vivo* applications have been limited by the relatively low absorption displayed by nanotubes at near-infrared region (NIR) and concerns over toxicity. Recently, golden carbon have been strategically designed and synthesized by depositing a thin layer of gold around the CNTs for photoacoustic and photothermal imaging *in vivo* [17]. The gold layer acts as an NIR absorption enhancer and could potentially address the issues of toxicity. Nevertheless, controllable synthesis of golden carbons is still a challengeable task, so developing a simple and effective method for prepared an NIR absorption enhancer CNTs has become a hotspot.

Gold nanorods (GNRs), strongly light enhanced absorption in NIR and plasmon resonance enhanced properties, are attracting intensive scientific interest for their unique properties and potential applications such as photothermal therapy [18], biosensing [19], molecular imaging [20], and gene delivery [21] for cancer treatment. However, the toxicity derived from a large amount of the surfactant cetyltrimethylammonium bromide (CTAB) during GNRs synthesis severely limits their biomedical applications [22-26]. Upon that, the biocompatible silica is chosen to modify the GNRs and removal of CTAB molecules on the surface of GNRs.

Herein, we demonstrate a simple and effective strategy for fabricating an NIR absorption enhancer CNTs through covalent interaction of carboxyl groups on the MWNT with the amino silane coupling agent modified silica-coated gold nanorods (sGNRs) as shown in Scheme 1. GNRs were prepared by the seed-mediated template-assisted protocol, coated by silica and modified with



Scheme 1. Covalent attachment of sGNRs on the MWNT surface.

the amino silane coupling agent, thus eliminating their cytotoxicity and improving their biocompatibility. Our results showed that the resulting MWNT/sGNRs have markedly NIR absorption enhancer.

## 2. Materials and Methods

### 2.1 Materials

Multiwalled carbon nanotubes (MWNTs) were purchased from the Shenzhen Nanoport Company (Shenzhen, China) and their diameters were around 20~30 nm. Chloroauric acid ( $\text{HAuCl}_4 \cdot 3\text{H}_2\text{O}$ ), Cetyltrimethylammonium bromide (CTAB), sodium borohydride ( $\text{NaBH}_4$ ), Tetraethylorthosilicate (TEOS), 3-aminopropyltrimethoxysilane (APTS), 1-ethyl-3-(3-dimethyl aminopropyl) carbodiimide (EDC), N-hydroxysuccinimide (NHS) and ascorbic acid were obtained from the Aldrich Company. Anhydrous ethanol and ammonium hydroxide were obtained from Sinopharm Co. (China).

### 2.2 Preparation of MWNT-COOH from MWNT (Scheme 1)

Crude MWNT were added to aqueous  $\text{HNO}_3$  (20.0 mL, 60%). The mixture was sonicated for 40 min and then stirred for 48 h while being boiled under reflux. The mixture was then vacuum-filtered through a 0.22 mm Millipore polycarbonate membrane and subsequently washed with distilled water until the pH of the filtrate was ~7. The filtered solid was dried at 70°C for 24 h in vacuum oven, yielding MWNT-COOH [27].

### 2.3 Synthesis of silica-modified gold nanorods

In a typical experiment, GNRs were synthesized according to the seed-mediated template-assisted protocol [19,28]. Twenty milliliters of the GNRs solution was

centrifuged at 9600 rpm for 15 min. The supernatant, containing mostly CTAB molecules, was removed and the solid (containing rods) was redispersed in 20 mL anhydrous ethanol adjusted to pH=10 with ammonia. After the system was sonicated for 30 min, TEOS of 4 mL (10 mM) was added and then the entire system was stirred for 20 h. Next, 10 mL APTS were added to form a mixed solution and allowed to react at 80°C for 3 h. The resultant was washed with deionized water for several times, and dried at 60°C for 3 h in vacuum oven to obtain the sGNRs.

### 2.4 Fabrication of MWNT/sGNRs nanohybrid (Scheme 1)

Covalent attachment of sGNRs to the MWNT was performed using a modification of the standard EDC-NHS reaction as described by Jönsson et al [29]. Carboxyl groups on the surface of MWNT (5 mg) were activated by an EDC/NHS solution for 30 min. Following activation, 1 mg sGNRs were added to form a mixed solution and allowed to react at room temperature for 12 h. The resultant was treated by high speed centrifugal separation and washed with deionized water for several times, then dried at 60°C for 3 h in vacuum oven to obtain the MWNT/sGNRs nanohybrid.

### 2.5 Characterization

JEOL JEM-2010 transmission electron microscope (TEM) and a JEOL JEM-2100F high-resolution transmission electron microscope (HR-TEM) were used to confirm particle size and observe the interface and the binding-site of sGNRs and MWNT. UV-vis spectra were measured at 20°C with a Shimadzu UV-2450 UV-visible spectrophotometer equipped with a 10-mm quartz cell, where the light path length was 1 cm. The 200~1000 nm wavelength region was scanned, since it includes

the absorbance of the GNRs. The fourier transform infrared (FTIR) spectra were recorded on a Perkin Elmer Paragon-1000 FTIR Spectrometer. The surface charge of MWNT/sGNRs was measured with Zeta potential measurements in water (NICOMP 380ZLS Zeta potential/Particle sizer).

### 3. Results and discussion

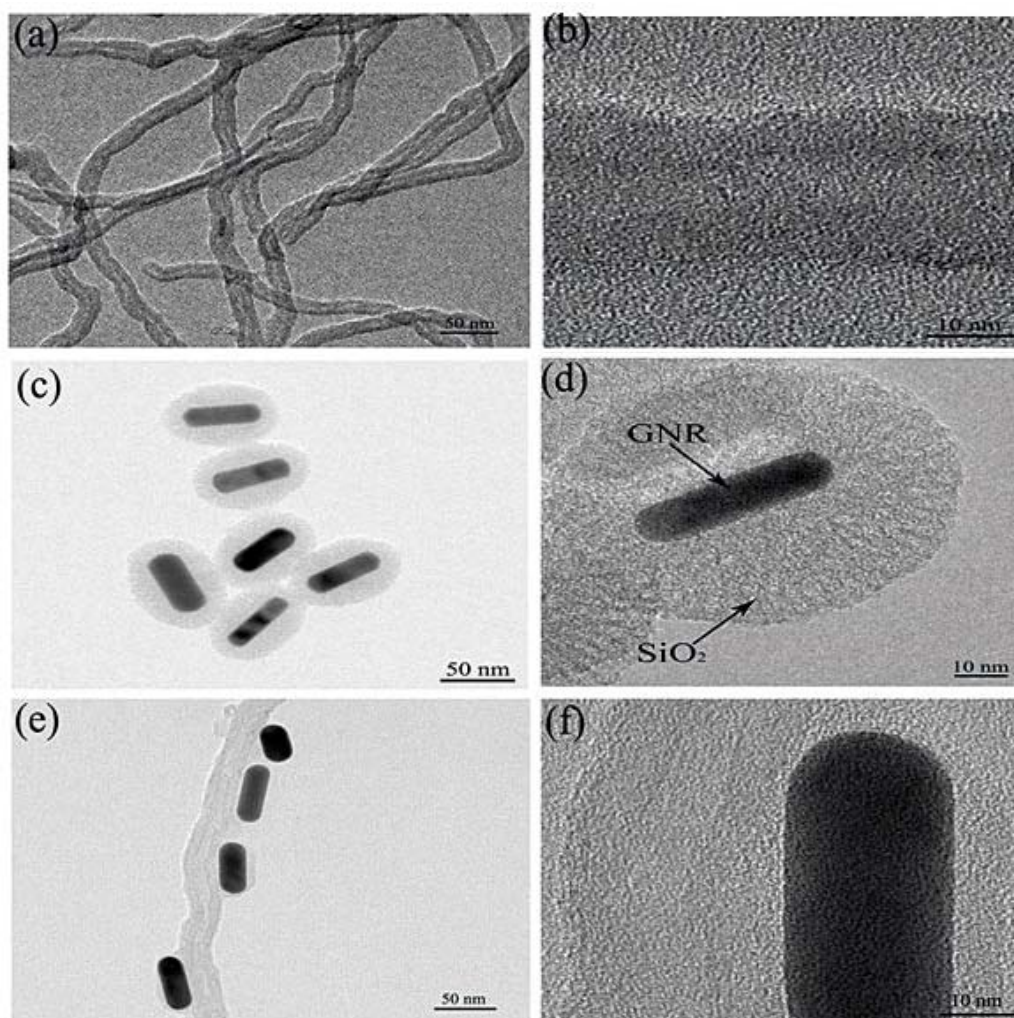
#### 3.1 TEM observation

Figure 1 displays typical TEM images and HR-TEM images of (a,b) MWNT, (c,d) sGNRs, (e,f) MWNT/sGNRs. As shown in Figure 1(a), MWNT used are relatively pure almost containing no amorphous carbon particles, metal catalysts or other impurities. The average diameter is around  $\sim 20$  nm. Thorough high resolution HR-TEM characterizations revealed the highly crystalline nature of MWNT in Figure 1(b), Figure 1(c) shows the morphology and the size distribution of silica-coated GNRs, indicating GNRs were fully encapsulated by silica. It can be seen that the sGNRs are approximate sphere with size about  $\sim 80$  nm. Moreover, the sGNRs with well-defined core-shell structures are rather monodisperse. The GNRs core, with 50 nm in length and 20 nm in

width, was prepared by seed-mediated template-assisted protocol. The silica shell has a thickness of 10–20 nm. Figure 1(d) is the HR-TEM of an individual sGNR. It indicated that the silica shell is well-ordered mesopore structure, which can be used as drug carrier, gene carrier, and gas adsorption and so on. It is easy to directly observe the sGNRs decorate the surface of MWNT mainly along their sidewalls from Figure 1(e) and (f), thus suggesting that functionalization of the MWNTs with sGNRs was successful. The well-distributed sGNRs deposited onto the MWNT demonstrate that the CNT pretreatment processing was effective, which resulted in many active sites on the carbon nanotubes, Figure 1(f) showed that the structure and the crystallinity of MWNT and sGNRs have no change after crosslink.

#### 3.2 Binding sites of sGNRs and MWNT

Low magnification TEM images of MWNT/sGNRs is shown in Figure 2(a,b) and high magnification TEM images of the different binding-site of sGNRs and MWNT in Figure 2(c,d). According to the TEM observations in Figure 2(a,b), sGNRs decorate the surface of MWNT mainly along their sidewalls, and partly connected to the nanotubes ends, which may be contributed to that the



**Figure 1** TEM images and HR-TEM images of (a,b) MWNT, (c,d) sGNRs, (e,f) MWNT/sGNRs.

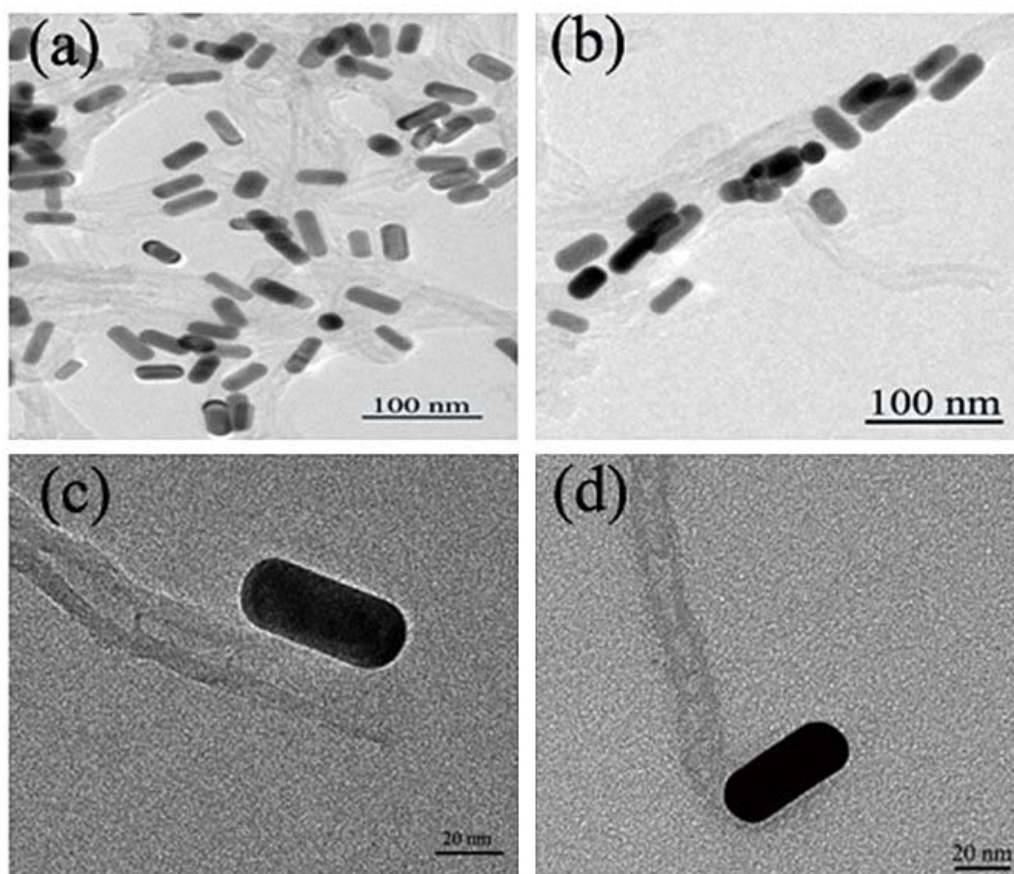


**Figure 2** TEM images of the different binding-site of sGNRs and MWNT.

amount of aminon groups on the long axis of GNRs is more than the amount on the short axis of GNRs. The typical sidewalls-decoration is displayed in Figure 2c, and the typical ends-decoration in Figure 2d. It indicated that the active sites (carboxyl groups) are fully on the sidewalls and ends of MWNT.

### 3.3 UV-vis spectra

Figure 3(A) shows the UV-vis absorbance spectra of GNR-CTAB, GNR-SiO<sub>2</sub> and sGNRs in the 400~900 nm wavelength range. The spectrum of GNR-CTAB showed that GNR-CTAB have two absorption bands, a weak short-wavelength band around 515 nm and a strong long-wavelength band around 715 nm. Moreover, we found that the plasmon peaks of sGNRs exhibited no significant changes in peak width or position, so the silica modification had no effect on the property and application of GNRs. After modified with amino silane coupling agent, the special absorption peaks have a little red shift (~6 nm), which may be contributed to that the coated silica layer turn thick and the size of sGNRs become big.

Figure 3(B) shows the UV-vis absorbance spectra of MWNT and MWNT/sGNRs. It can be seen that MWNTs have the relatively low absorption displayed at NIR. After covalent binding of sGNRs, the MWNT/sGNRs display markedly NIR absorption enhancer. The inset shows the magnification absorbance spectra of MWNT/sGNRs in the region of 400~800 nm, there are two special absorption peaks corresponding to sGNRs.

### 3.4 FTIR spectroscopy

To further study for covalently attaching sGNRs onto the surface of MWNT, the typical FT-IR spectra of (a) MWNT, (b) sGNRs, and (c) MWNT/sGNRs were determined in Figure 4. The presence of sGNRs can be seen by a strong absorption bands at around 1060 cm<sup>-1</sup>. In addition, in Figure 4(a) and (b) the absorption bands near 3400 and 1630 cm<sup>-1</sup> refer to the vibration of remainder H<sub>2</sub>O in the samples. The fact was proven by comparison of FT-IR spectra of the MWNT and MWNT/sGNRs nanohybrids shown in Figure 4(a) and (c). The difference between the IR spectrum of MWNT and that of MWNT/sGNRs is obvious. The bands Si-O at 1061 cm<sup>-1</sup> indicated the silica in (c), but it wasn't found in (a). Covalent attachment of sGNRs to MWNTs surface is verified by pronounced amide I and III vibrational stretches (1641 and 1462 cm<sup>-1</sup>, respectively, Figure 4(insert)). These changes in FT-IR absorption spectroscopy can be explained by the covalent interaction between sGNRs and MWNTs.

### 3.5 Zeta potential Analysis

Zeta potentials of MWNT/sGNRs with increasing sGNRs concentration were recorded at pH=7.0 as shown in Figure 5. As demonstrated in Figure 5, MWNT/sGNRs nanocomposites all bear negative charge. The value of negative charge was decreased depending highly on concentration of sGNRs added in the reaction system, which is attributed to that the number of carboxyl groups

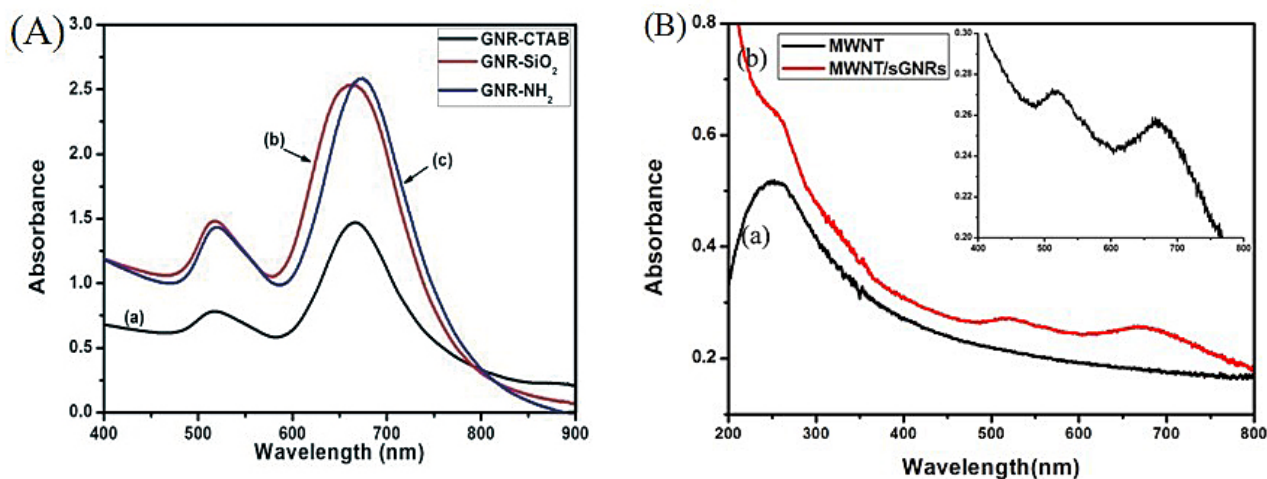


**Figure 3** (A) UV-vis spectra of (a) GNR-CTAB, (b) GNR-SiO<sub>2</sub>, and (c) GNR-NH<sub>2</sub>. (B) UV-vis spectra of (a) MWNT and (b) MWNT/sGNRs (The inset shows the magnification in the region of 400~800 nm).

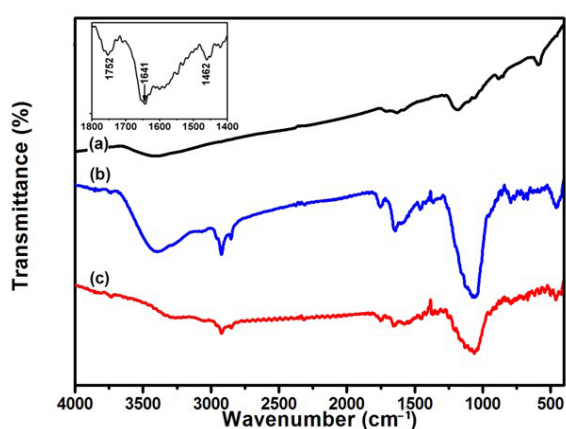


**Figure 4** FTIR spectra of (a) MWNT, (b) sGNRs, and (c) MWNT/sGNRs (The inset shows the magnification in the region of 1400~1800 cm<sup>-1</sup>).

on the surface of MWNT was decreased. It may be also contribution to the enrichment of hydroxy groups on the silica surface of sGNRs. In addition, the negative charge depicted that the MWNT/sGNRs have good dispersity.

#### 4. Conclusions

In summary, we have developed a simple and effective strategy for functionalization of carbon nanotubes with gold nanorods by covalent interaction. The MWNT/sGNRs shows an excellent solubility and good dispersity in aqueous solution and display markedly absorption enhancer in the near-infrared region. Therefore, the novel hybrid nanostructure should open up new possibilities in nanomedicine as multimodal photoacoustic and photothermal high-contrast molecular agent. It also has great potential applications in advanced sensing, nanoelectronics, chemical sensing, field-emission displays, nanotribology, cell adhesion/biorecognition investigations, and catalytic systems.

#### Acknowledgements

This work is supported by the National Key Basic Research Program (973 Project) (2010CB933901), National 863 Hi-tech Project

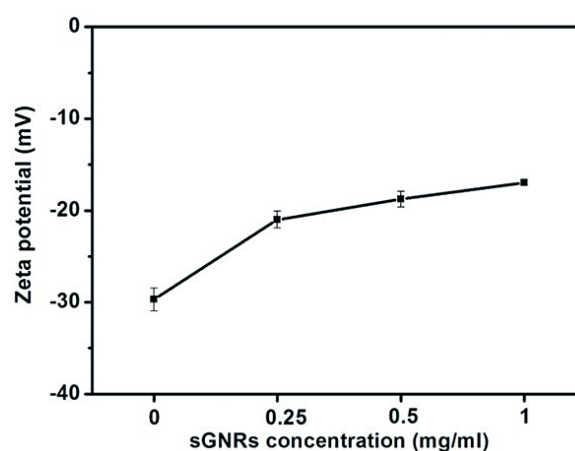


**Figure 5** Zeta potentials of MWNT/sGNRs with increasing sGNRs concentration.

(2007AA022004), Important National Science & Technology Specific Projects (2009ZX10004-311), National Natural Scientific Fund (No.20771075 and 20803040), Special project for nano-technology from Shanghai (No.1052nm04100), New Century Excellent Talent of Ministry of Education of China (NCET-08-0350), Shanghai Science and Technology Fund (10XD1406100), Doctoral Program of Higher Education Research Fund(20070248050, 20070248107), and Shanghai Jiao Tong University Innovation Fund For Postgraduates.

#### References

- Peng X, Wong S. Functional covalent chemistry of carbon nanotube surfaces. *Adv. Mater.* 2008;21:625-642. doi:10.1002/adma.200801464
- Wong S, Joselevich E, Woolley A, Cheung C, Lieber C. Covalently functionalized nanotubes as nanometre-sized probes in chemistry and biology. *Nature* 1998;394:52-55. doi:10.1038/27873
- Hu X, Dong S. Metal nanomaterials and carbon nanotubes-synthesis, functionalization and potential applications towards electrochemistry. *J. Mater. Chem.* 2008;18:1279-1295. doi:10.1039/b713255g
- Bottini M, Tautz L, Huynh H, Monosov E, Bottini N, Dawson M, et al. Covalent decoration of multi-walled carbon nanotubes with silica nanoparticles. *Chem. Commun.* 2005;758-760. doi:10.1039/b412876a
- Deng Y, Deng C, Yang D, Wang C, Fu S, Zhang X. Preparation, characterization and application of magnetic silica nanoparticle functionalized multi-walled carbon nanotubes. *Chem. Commun.* 2005; 5548-5550. doi:10.1039/b511683j
- Pan B, Cui D, Gao F, He R. Growth of multi-amine terminated poly (amidoamine) dendrimers on the surface of carbon nanotubes. *Nanotechnology* 2006;17:2483- 2489. doi:10.1088/0957-4484/17/10/008
- Wang Z, Li M, Zhang Y, Yuan J, Shen Y, Niu L, et al. Thionine-

- interlinked multi-walled carbon nanotube/gold nanoparticle composites. *Carbon* 2007;45:2111-2115. doi:10.1016/j.carbon.2007.05.018
8. Pan B, Cui D, He R, Gao F, Zhang Y. Covalent attachment of quantum dot on carbon nanotubes. *Chem. Phys. Lett.* 2006;417:419-424. doi:10.1016/j.cplett.2005.10.044
  9. Xu P, Cui D, Pan B, Gao F, He R, Li Q, et al. A facile strategy for covalent binding of nanoparticles onto carbon nanotubes. *Appl. Surf. Sci.* 2008;254:5236-5240. doi:10.1016/j.apsusc.2008.02.082
  10. Pan B, Cui D, Xu P, Ozkan C, Feng G, Ozkan M, et al. Synthesis and characterization of polyamidoamine dendrimer-coated multi-walled carbon nanotubes and their application in gene delivery systems. *Nanotechnology* 2009;20:125101. doi:10.1088/0957-4484/20/12/125101
  11. Chen D, Wu X, Wang J, Han B, Zhu P, Peng C. Morphological Observation of Interaction between PAMAM Dendrimer PAMAM Dendrimer Modified Single Walled Carbon Nanotubes and Pancreatic Cancer Cells. *Nano Biomed. Eng.* 2010;2:61-66. doi:10.5101/nbe.v2i1.p61-66
  12. Liu C. Research and Development of Nanopharmaceuticals in China. *Nano Biomed. Eng.* 2009;1:1-12. doi:10.5101/nbe.v1i1.p1-12
  13. De La Zerda A, Zavaleta C, Keren S, Vaithilingam S, Bodapati S, Liu Z, et al. Carbon nanotubes as photoacoustic molecular imaging agents in living mice. *Nat. Nanotechnol.* 2008;3:557-562. doi:10.1038/nnano.2008.231
  14. Kam N, O'Connell M, Wisdom J, Dai H. Carbon nanotubes as multifunctional biological transporters and near-infrared agents for selective cancer cell destruction. *Proc. Natl. Acad. Sci. U. S. A.* 2005;102:11600. doi:10.1073/pnas.0502680102
  15. Zharov V, Galanzha E, Shashkov E, Kim J, Khlebtsov N, Tuchin V. Photoacoustic flow cytometry principle and application for real-time detection of circulating single nanoparticles, pathogens, and contrast dyes contrast dyes in vivo. *J. Biomed. Opt.* 2007;12:051503. doi:10.1117/1.2793746
  16. Kim J, Shashkov E, Galanzha E, Kotagiri N, Zharov V. Photothermal antimicrobial nanotherapy and nanodiagnostics nanodiagnostics with self-assembling carbon nanotube clusters. *Lasers Surg. Med.* 2007;39:622-634. doi:10.1002/lsm.20534
  17. Kim J, Kotagiri N, Kim J, Deaton R. In situ fluorescence microscopy visualization and characterization of nanometer-scale carbon nanotubes labeled with 1-pyrenebutanoic acid, succinimidyl ester. *Appl. Phys. Lett.* 2006;88:213110. doi:10.1063/1.2206875
  18. Cui D, Li Z, Huang P, Zhang X, Lin J, Yang S, et al. RGD-conjugated dendrimer-modified gold nanorods for in vivo tumor targeting and photo-thermal therapy. *Mol. Pharm.* 2009; 7:94-104 doi: 10.1021/mp9001415
  19. Zhu Z, Tang Z, Phillips J, Yang R, Wang H, Tan W. Regulation of singlet oxygen generation using single-walled carbon nanotubes. *J. Am. Chem. Soc.* 2008;130:10856-10857. doi:10.1021/ja802913f
  20. von Maltzahn G, Centrone A, Park J, Ramanathan R, Sailor M, Hatton T, et al. SERS-coded gold nanorods as a multifunctional platform for densely multiplexed near-infrared imaging and photothermal heating. *Adv. Mater.* 2009;21:3175. doi:10.1002/adma.200803464
  21. Chen S, Ji Y, Lian Q, Wen Y, Shen H, Jia N. Gold Nanorods Coated with Multilayer Polyelectrolyte as Intracellular delivery Vector of Antisense Oligonucleotides. *Nano Biomed. Eng.* 2010;2:15-23.
  22. Huang X, El-Sayed I, Qian W, El-Sayed M. Cancer cells assemble and align gold nanorods conjugated to antibodies to produce highly enhanced, sharp, and polarized surface Raman spectra: A potential cancer diagnostic marker. *Nano Lett.* 2007;7:1591-1597. doi:10.1021/nl070472c
  23. Wijaya A, Hamad-Schifferli K. Ligand customization and DNA functionalization of gold nanorods via round-trip phase transfer ligand exchange. *Langmuir* 2008;24:9966-9969. doi:10.1021/la8019205
  24. Orendorff C, Alam T, Sasaki D, Bunker B, Voigt J. Phospholipid- Gold Nanorod Composites. *ACS nano* 2009;3:971-983. doi:10.1021/nm900037k
  25. Huang P, Li Z, Lin J, Cui D. Preparation of surface dendrimer-modified gold nanorods by round-trip phase transfer ligand exchange. *J. Phys.: Conf. Ser.* 2009;188:012031. doi: 10.1088/1742-6596/188/1/012031.
  26. Yang D, Cui D. Advances and Prospects of Gold Nanorods. *Chem.-Asian J.* 2008;3:2010-2022. doi:10.1002/asia.200800195
  27. Xu Y, Gao C, Kong H, Yan D, Jin Y, Watts P. Growing multihydroxyl hyperbranched polymers on the surfaces of carbon nanotubes by in situ ring-opening polymerization. *Macromolecules* 2004;37:8846-8853. doi:10.1021/ma0484781
  28. Pan B, Cui D, Ozkan C, Xu P, Huang T, Li Q, et al. DNA-templated ordered array of gold nanorods in one and two dimensions. *J. Phys. Chem. C* 2007;111:12572-12576. doi:10.1021/jp072335+
  29. Jansson U, Fgerstam L, Ivarsson B, Johnsson B, Karlsson R, Lundh K, et al. Real-time biospecific interaction analysis using surface plasmon resonance and a sensor chip technology. *Biotechniques* 1991; 11:620.

Received 10 November, 2010; accepted 6 December, 2010; published online 16 December, 2010.

**Copyright:**(c) 2010 P. Huang, et al. This is an open-access article distributed under the terms of the Creative Commons Attribution License, which permits unrestricted use, distribution, and reproduction in any medium, provided the original author and source are credited.